



Evolution characteristics of precursor information of coal and gas outburst in deep rock cross-cut coal uncovering

Jupeng Tang¹ · Xin Zhang¹ · Shengjie Sun¹ · Yishan Pan² · Liping Li¹

Received: 24 March 2021 / Accepted: 17 January 2022
© The Author(s) 2022

Abstract

As mines become deeper, the potential for coal and gas outbursts in deep rock cross-cut coal uncovering is enhanced. The outburst precursors are unclear, which restricts the effectiveness and reliability of warning systems. To reveal the evolution characteristics of coal and gas outburst precursor information in deep rock cross-cut coal uncovering, briquette specimens are constructed and experiments are conducted using a self-developed true triaxial outburst test system. Using acoustic emission monitoring technology, the dynamic failure of coal is monitored, and variations in the root mean square (RMS) of the acoustic emissions allow the effective cracking time and effective cracking gas pressure to be defined. These characteristics are obviously different in deep and shallow coal. The characteristic parameters of gas outburst exhibit stepwise variations at different depths. The RMS and cumulative RMS have stepped failure characteristics with respect to changes in gas pressure. The characteristic parameters of coal failure are negatively correlated with the average in-situ stress and effective stress, but positively correlated with the lateral pressure coefficient of in-situ stress and the critical gas pressure. The transition characteristics are highly sensitive in all cases. The critical depth between deep and shallow coal and gas outbursts is 1700 m. The expansion multiple of acoustic emission intensity from the microfracture stage to the sharp-fracture stage of coal is defined as the outburst risk index, N_1 . For depths of 1100–1700 m, $N_1 \geq 7$ denotes a higher risk of outburst, whereas at depths of 1700–2500 m, $N_1 \geq 3$ indicates enhanced risk.

Keywords Deep coal and gas outburst · Rock cross-cut coal uncovering · Acoustic emission · Critical gas pressure · Risk index

1 Introduction

Coal and gas outbursts are the most harmful dynamic coal mine disasters in China, seriously threatening the safety of underground workers (Chen et al. 2014; Wu et al. 2020; Wang and Meng 2018; Cao et al. 2019, 2020; Ma et al. 2020a). Among the various outburst accidents that have occurred, the average strength of the outbursts induced by rock cross-cut coal uncovering is more than six times that of other accidents, and more than 80% of outbursts are induced

by rock cross-cut coal uncovering (Jiang 2015; Xie and Feng 2011; Yang et al. 2021). However, there is little information about the precursors of coal outbursts. To avoid an outburst in the process of rock cross-cut coal uncovering, it is necessary to measure the outburst risk index accurately and take appropriate preventive measures (Ma et al. 2020b; Fu et al. 2019). Therefore, exploring the precursor information is vital in the process of rock cross-cut coal uncovering.

In China, research on predicting the outburst risk for crosscuts began in the 1970s. Since then, many forecasting methods have been proposed, including the single index, comprehensive index, and desorption index of the drill cutting method (Xu et al. 2012). Alekseev et al. (1980) used a triaxial loading system for coal and gas outburst experiments and analyzed the outburst conditions under different stresses. Singh (1984) conducted experiments and theoretical analysis, and described the action and interaction of geological factors and mining factors in coal and gas outbursts. Based on the theory of mechanics, Hu et al. (2008) conducted

✉ Xin Zhang
LntuZx0812@163.com

¹ School of Mechanics and Engineering, Collage of Mechanics Engineering, Liaoning Technical University, No. 47, Zhonghua Road, Xihe District, Fuxin City 123000, Liaoning Province, China

² School of Physics, Liaoning University, Shenyang 110036, Liaoning, China

detailed analysis of the various stages of coal fracture and deformation during the whole process of coal and gas outburst. The mechanical properties of the surrounding rock and the changes in outburst risk during the process of uncovering coal have also been analyzed (Hu et al. 2012). Peng et al. (2012) indicated that the gas seepage decreases the strength of coal containing gas and accelerates its failure process. The laws of gas occurrence, the intensity of the coal outburst, and the regional partition have been studied by Wang et al. (2013) and Guo et al. (2020). Xue et al. (2015) studied the cracking of coal under compressive stress conditions and the permeability variations during the whole process. They found that the coal failure and degradation of mechanical properties were essentially related to the propagation and coalescence of induced cracks. Yu et al. (2015) believed that the gas dilatation energy was the main energy source for outburst events, and showed that an energy index could reflect the possibility of coal seam outbursts. Zhao et al. (2019) believed that the principal stress ratio and the strength of the coal rock mass were significantly affected by the size of the plastic zone during the process of rock cross-cut coal uncovering. The outburst process has been investigated by analyzing the gas pressure variation, temperature variation, outburst propagation velocity, particle size of outburst coal, and energy transformation (Nie et al. 2019). Yuan et al. (2020) carried out similar simulation experiments on coal and gas outbursts induced by uncovering coal in cross-cuts during roadway excavation, and obtained parameters related to the quality, distance, hole location, and shape of the outburst coal powder. Zhang et al. (2021) analyzed the ejected coal and, based on a new surface theory, developed an outburst fragmentation index that can be linearly fitted to the relative intensity of the outburst. The fitting parameters k and a reflect the intensity of the outburst and the degree of difficulty in the occurrence of outburst, respectively. Based on the η prediction method, a new method for coal and gas outburst prevention was specified. Liu et al. (2018) used COMSOL to simulate and analyze the stress and gas pressure during the process of rock cross-cut coal uncovering, and analyzed the influence of stress and gas pressure on coal and gas outbursts from an energy perspective. The gas drainage performance in coal seams with different combinations of tectonically deformed sub-layers and intact sub-layers was recently numerically analyzed by Zhao et al. (2020). Heo et al. (2004) explored the acoustic emission characteristics of the rock sample fracture process by loading different paths of confining pressure and stress in experiments. The micro-seismic and acoustic emission effects of an abnormal gas outburst triggered by a strong rock burst were thoroughly investigated using appropriate monitoring systems and spectral analysis by Lu et al. (2014).

The above-mentioned research indicates that many scholars have investigated the precursor information and outburst

risk indicators of coal and gas outbursts. However, there has been no discussion on the characteristics of the deep coal outburst process and the precursor warning indicators from the perspective of acoustic emission energy conversion. Using a self-developed true triaxial coal and gas outburst simulation test device, this study conducted outburst simulation experiments on coal samples from Hongyang No. 3 mine, which is an outburst coal seam with a current mining depth of 1100 m. Based on the dual parameters of the acoustic emission signal and the gas pressure, a risk index for deep coal and gas outburst is established. The variation of influence of the average in-situ stress, lateral pressure coefficient of in-situ stress, critical gas pressure, and effective stress on the coal failure characteristic parameters is explored, and new principles are provided for deep coal and gas outburst.

2 Experimental device and scheme design

Outburst induced by rock cross-cut coal uncovering is a complex dynamic gas disaster that is common during the coal mining process. It is difficult to observe in the field and can be extremely dangerous. Therefore, studying the precursor characteristics of coal and gas outburst using a laboratory-based experiment simulation method is of great significance.

2.1 Experimental and monitoring system

A coal and gas outburst simulation experimental system was developed. The test device system shown in Fig. 1 includes a true triaxial experimental system, acoustic emission monitoring system, pressure and in-situ stress loading system, and data acquisition control system.

The main structure of the true triaxial experimental system is composed of 200-tonnes upper and lower end presses, hydraulic pump platforms, and hydraulic consoles. The internal cavity of the experimental system, which is where the pulverized coal is pressed, measures 200 mm × 200 mm × 220 mm. The pulverized coal is directly pressed into shape by the upper end press, and the maximum molding pressure can reach 30 MPa. Through the three-dimensional separate loading and unloading system, the true triaxial stress loading of the test specimen can be realized. The maximum loading pressure is 25 MPa, and the cylinder loading stroke is 20 mm. There are a total of 24 gas injection and discharge ports and various sensor interfaces on the four sides of the model. These measure the changes of stress, sound, and electrical signals in the model cavity. The front face of the model allows a circular coal and gas outburst with a diameter of 80 mm through a plexiglass baffle, which simulates the weak surface and induces coal and gas outburst. The plexiglass is fixed and sealed with a

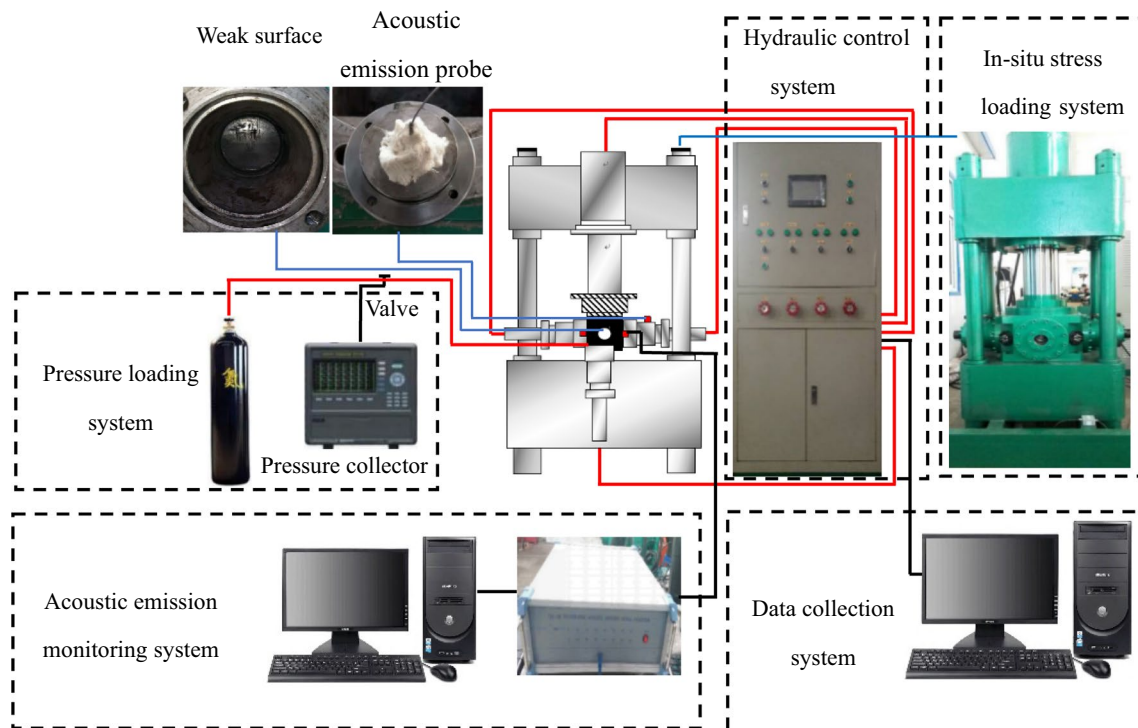


Fig. 1 Coal and gas outburst testing system (red lines: pipe connections, black lines: wires, blue lines: guide lines)

pressure plate and a sealing rubber ring. When the internal gas pressure of the coal reaches the critical pressure, the plexiglass baffle is destroyed and the coal body is sprayed out under the gas pressure, realizing the on-site simulation of coal and gas outburst.

The test device has the following advantages:

- (1) The determination of the outburst coal size is based on analysis of typical outburst cases. The size, shape, and volume are reasonable, and most coal and gas outburst cases can be simulated.
- (2) The experimental device has a variety of data acquisition channels, which can collect and save the sound, electricity, force, and other parameter information generated by changes in the coal structure at each stage of loading.
- (3) The device can truly simulate deep in-situ stress loading, that is, the vertical in-situ stress, maximum horizontal in-situ stress, and minimum horizontal in-situ stress are simultaneously loaded in three directions.
- (4) During the experiments, the coal samples are removed after molding, which ensures the desired initial mechanical properties of the specimen. At the same time, this is conducive to the sealing of the device, making the simulations more realistic and effective.
- (5) The plexiglass baffle at the outburst mouth enables the coal and gas outburst to be naturally induced, rather

than forcing an outburst to become active when the critical conditions are reached.

This study mainly uses acoustic emission monitoring technology, which monitors the internal failure of the coal during the coal and gas outburst process. A DS5-16B full-information acoustic emission signal monitoring analyzer is used. This analyzer can extract the characteristic parameters of the acoustic emissions and waveform data in real time during the experiments.

2.2 Design of experimental scheme

The coal samples used for the experiments were collected from the 12th coal seam in the outburst mine of Hongyang No. 3 Mine, operated by the Shenyang Coking Coal Co., Ltd. Table 1 presents data related to the coal seams. The specific experimental steps were as follows: (1) The selected coal was rolled several times to produce a powder, and then sieved to obtain five different particle sizes of 20–40, 40–60, 60–80, 80–100, and > 100 μm ; (2) The coal powder was poured into the pressure chamber of the experimental equipment according to the theoretical ratio of the maximum density curve (Table 2), and pressed into shape with the upper end press. The pressed shape was not removed from the apparatus after molding; (3) The upper end of the press was pressed down to form a tight seal with

Table 1 Basic parameters of coal seam

Gas content (m/kg)	Water content (%)	Average thickness (m)	Coal seam density (g/cm ³)	Compressive strength (MPa)
15.1 × 10 ⁻³	5	1.89	1.38	6.94–9.04

the pressure chamber, and the experimental device was filled with nitrogen. The briquette adsorbed the nitrogen for 24 h until it was saturated; (4) The three-dimensional stress required for the actual experiment was applied (see Table 3). These stress values were taken from the “Coal Mine Safety Production Regulations”, which state that the critical gas pressure of coal and gas outburst is 0.74 MPa. Thus, the initial gas pressure of the experiment was set to 0.75 MPa, and the pressure was increased to 1 MPa after 2 min of stabilization. The pressure was increased in steps of 0.2 MPa with 2 min for pressure stabilization at each level until an outburst occurred; (5) The confining pressure and axial pressure loaded onto the briquette were adjusted to simulate outbursts of coal and gas at different depths. Finally, the results were analyzed and compared.

2.3 Experimental parameters

According to similarity theory (Tang et al. 2013), the stress ratio of raw coal to briquette is 12. Regarding the deep underground stress environment, Li et al. (2012) collected data from more than 600 mining areas in mainland China, and plotted the distribution of the deep underground stress with respect to depth. They found that:

$$\begin{aligned} \sigma_v &= 0.0208H + 2.195 \\ \sigma_H &= 0.0238H + 7.648 \\ \sigma_h &= 0.0184H + 0.948 \end{aligned} \tag{1}$$

where, H (m) denotes depth, σ_v (MPa) is vertical in-situ stress, σ_H (MPa) is the maximum horizontal in-situ stress, and σ_h (MPa) is the minimum horizontal in-situ stress.

According to the research results of Li et al. (2012), the actual in-situ stresses were defined for different depths. The experimental in-situ stress values were then determined according to the stress ratio of 12 (Table 3).

The experiments used briquette specimens. Following Tang (2006), the mass of coal powder was taken as 8.7 kg, giving a briquette density of 1.087 t/m³. To make the mechanical properties of the briquette specimens similar to those of raw coal, the molding pressure was set as 20 MPa. The initial gas pressure was 0.75 MPa, and the staged loading method was used to improve the similarity of the specimens. The stabilization time was 30 min. The proportions of the eight groups of experiment coal powders are listed in Table 2. To enhance the strength of the specimens, a small amount of plaster was mixed with the coal powder as a binder when the briquettes were pressed.

2.4 Analysis of experimental phenomena

Considering coal and gas outbursts at different depths, eight groups of experiments were conducted under different axial and confining pressure loading conditions. The experimental results are presented in Table 4. During the outburst, the coal carries gas and spews out violently in a trumpet shape, accompanied by a violent loud noise. The outburst lasts for 0.6–1.8 s. The ejected coal and gas have a large

Table 2 Ratio scheme of briquettes

Project	Parameter					
Particle size (μm)	20–40	40–60	60–80	80–100	> 100	Plaster
Mass ratio (%)	29.3	16.5	8.2	4	37	5

Table 3 Experimental scheme of coal and gas outburst

Test depth (m)	Actual in-situ stress (MPa)			Experimental in-situ stress (MPa)		
	σ_H	σ_h	σ_v	σ_H'	σ_h'	σ_v'
1100	33.83	21.19	25.08	2.82	1.77	2.09
1300	38.59	24.87	29.24	3.22	2.07	2.44
1500	43.35	28.55	33.40	3.61	2.38	2.78
1700	48.11	32.23	37.56	4.01	2.69	3.13
1900	52.87	35.91	41.72	4.41	2.99	3.48
2100	57.63	39.59	45.88	4.80	3.30	3.82
2300	62.39	43.27	50.04	5.20	3.61	4.17
2500	67.15	46.95	54.20	5.60	3.91	4.52

Table 4 Experimental results of outburst

Depth (m)	Total coal mass (g)	Outburst coal mass (g)	Relative outburst intensity (%)	Critical gas pressure (MPa)	Time (s)
1100	8700	7665	88.10	3.66	1743
1300		7607	87.44	3.48	1640
1500		7568	86.99	3.05	1403
1700		7444	85.56	2.87	1283
1900		7437	85.48	2.84	1273
2100		7334	84.30	2.76	1227
2300		7298	83.89	2.65	1187
2500		7194	82.69	2.47	1069

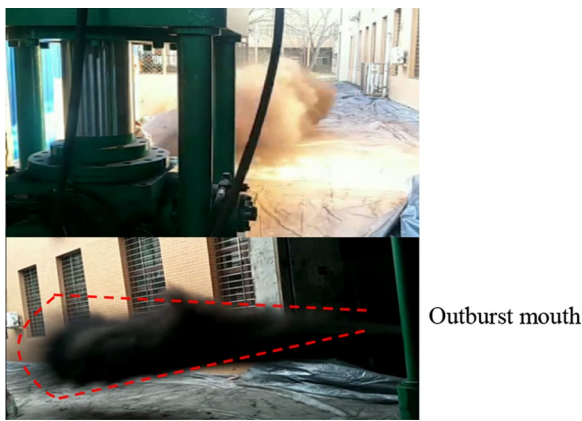


Fig. 2 Similar simulation site of outburst

initial velocity and form a coal–gas storm flow (Zhou et al. 2020). The kinetic energy is gradually exhausted as the debris is sprayed over an area of 20–25 m², and the coal powder spreads under the action of inertia and atmospheric pressure. The outburst can reach distances of 25 m. During the outburst, the coal undergoes secondary crushing, resulting in a large amount of coal dust. This can drift and sink over distances of 30 m under the action of the protruding air flow (Fig. 2).

Figure 3 shows that an increase in depth reduces the relative outburst intensity. As the depth increases from 1100 to 2500 m, the relative intensity decreases from 88.10% to 82.69%, and the critical gas pressure decreases from 3.66 to 2.47 MPa. For depths between 1100 and 1700 m, the relative outburst intensity and critical gas pressure drop sharply—the reduction rates in the relative outburst intensity and critical gas pressure are 4.23 and 1.32, respectively. From 1700–1900 m, the rate of decrease in the relative outburst intensity and critical gas pressure suddenly slows to around 1/10 of the decrease rate from 1100 to 1700 m. Over a depth range of 1900–2500 m, the relative outburst intensity and critical gas pressure decrease rate gradually increase to 4.65 and 0.62, respectively. This is because, as the depth increases, the stress conditions become more complicated. The in-situ stress gradually increases,

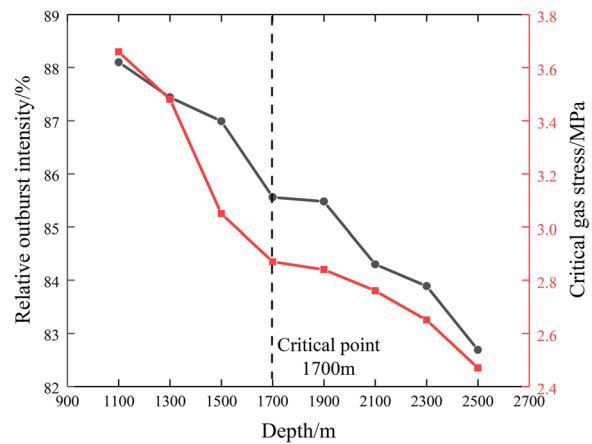


Fig. 3 Variation of relative outburst intensity and critical gas pressure with depth

meaning that the coal undergoes significant internal damage and the coal damage threshold is lowered. Therefore, it is easier to reach the critical gas outburst pressure, making it more likely that an outburst will occur, which is consistent with the actual situation on site. The gas internal energy is the main source of power for gas outburst (Li et al. 2019), but Tables 3 and 4 suggest that when a greater in-situ stress is imposed, the overall critical gas pressure decreases. This would appear to indicate that coal and gas outbursts are not only affected by the gas internal energy but are also influenced by factors such as the in-situ stress and the environment of the coal and its physical properties. This is consistent with the hypothesis of the combined effect of coal and gas outburst.

3 Evolution characteristics of gas outburst precursor information

When coal deforms or ruptures under force, cracks are formed in the coal seam, and the continuous expansion of these cracks is accompanied by the release of energy, mainly in the form of elastic waves, a phenomenon known

as acoustic emission. The purpose of acoustic emission monitoring is to determine the evolution characteristics of precursor acoustic emissions of coal and gas outbursts so as to predict the dynamic process of coal and gas outbursts.

3.1 Analysis of root mean square evolution characteristics

The acoustic emission signals collected in the tests are continuous, and thus enable the dynamic damage of the coal to be monitored during the outburst process. We select the root mean square (RMS) of the effective voltage as the acoustic emission parameter. The variation in the acoustic emission RMS and cumulative RMS with gas pressure loading at different depths is shown in Fig. 4.

The variations in the RMS and cumulative RMS can be analyzed as follows:

- (1) Under different depth conditions, the RMS and cumulative RMS changes with gas pressure exhibit significant differences, although there are obvious stepped and concentrated failure characteristics on the whole. As the gas pressure continues to increase, the coal damage exhibits transition characteristics, that is, there is a critical value (the critical point in Fig. 4) of the gas pressure during the coal and gas outburst process. When the gas pressure exceeds this critical value, the cumulative RMS shows a step-wise increase to a value that is much larger than in the initial stage of loading. This directly reflects the sharp increase in the number of new fractures in the coal and the destruction intensity at this stage.
- (2) During the coal and gas outburst tests, before the gas pressure is loaded, the three-dimensional in-situ stress loading conditions are set. Therefore, the acoustic emission signal mainly monitors the gas pressure in the tearing coal stage and the coal instability throwing stage. According to the variations in the acoustic emission RMS and cumulative RMS with gas pressure, the gas tearing coal process can be divided into two stages: microfracture and sharp-fracture stages. In the microfracture stage, the gas pressure is initially relatively small, and the tearing effect on the coal is limited, so the effective acoustic emission signals are not obvious. Only when the gas pressure is loaded can clear acoustic emission signals be captured, although the acoustic emission intensity remains generally low. The cumulative RMS growth is slow, there are few new cracks and little crack expansion, the volume of desorbed gas is small, and the self-increasing phenomenon of gas pressure is not obvious. At this time, the gas energy in the accumulation process is not sufficient to reach the release intensity. In the sharp-fracture stage,

once the cumulative amount of gas energy exceeds the intensity of the coal, effective acoustic emission signals continue to appear and the RMS level suddenly rises. This reflects the rapid destruction state inside the coal: the number of new cracks increases, the destruction intensity increases to form a cross-fracture network, and the gas adsorbed on the surface of the coal particles is released into the cracks to enhance the gas internal energy and promote crack expansion. These results are in agreement with the study of Jiang and Yu (1995).

3.2 Evolution of coal failure characteristic parameters

To study the degree of coal destruction during coal and gas outbursts, the characteristic parameters of coal destruction are taken to be the effective cracking time and the effective cracking gas pressure. We assume that the boundary time and gas pressure between the microfracture and sharp-fracture stages are the effective cracking time and the effective cracking gas pressure, as these values specifically reflect the time at which coal and gas outbursts become more likely to appear at different depths. As the depth and in-situ stress increase, the critical gas pressure gradually decreases. The in-situ stress and gas pressure directly affect the destruction of the coal, and are the main sources of power that cause the coal to enter the sharp-fracture stage. Therefore, exploring the relationship between the effective cracking time, effective cracking gas pressure, in-situ stress, critical gas pressure, and effective stress is of great significance for studying the risk of coal outburst and predicting coal and gas outbursts in advance. Under different depth conditions, the variation in the coal failure characteristic parameters is summarized in Table 5.

With increases in depth, the maximum horizontal in-situ stress, minimum horizontal in-situ stress, and vertical in-situ stress of the coal seam increase accordingly. Taking no account of the influence of in-situ stress in a single direction on the failure of the coal, the variations in the effective cracking time and effective cracking gas pressure are analyzed by means of the average in-situ stress and lateral pressure coefficient of in-situ stress.

The average in-situ stress and lateral pressure coefficient of in-situ stress are calculated using Eqs. (2) and (3), respectively.

$$\sigma_a = \frac{1}{3}(\sigma'_H + \sigma'_h + \sigma'_v) \quad (2)$$

where, σ_a (MPa) denotes the average in-situ stress, σ'_H (MPa) is the maximum horizontal in-situ stress applied in the test, σ'_h (MPa) is the minimum horizontal in-situ stress applied in the test, and σ'_v (MPa) is the vertical in-situ stress applied in the test.

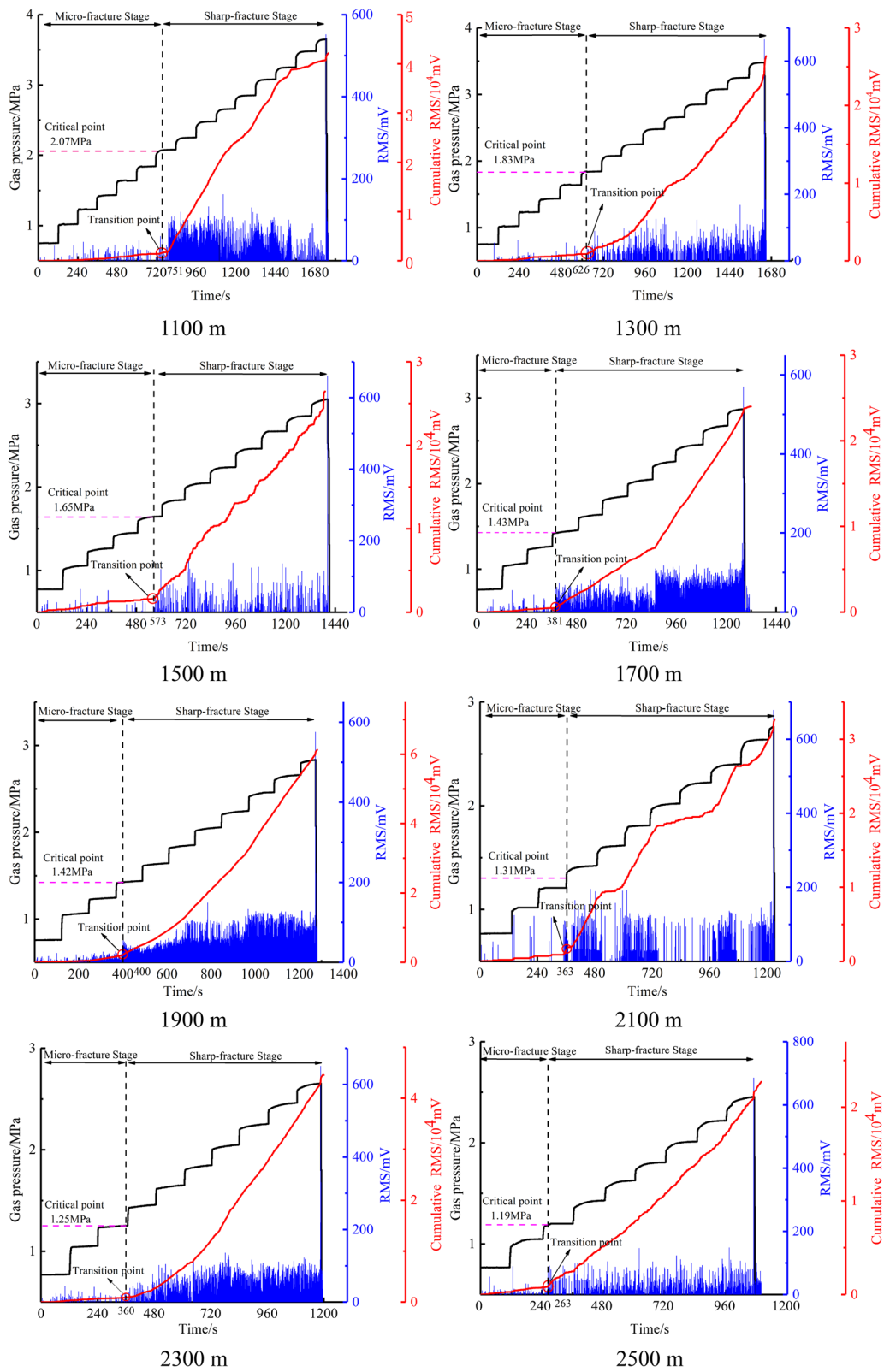


Fig. 4 Evolution of RMS and cumulative RMS with gas pressure at different depths

Table 5 Effective cracking time and effective cracking gas pressure of coal and gas outburst processes at different depths

Depth (m)	1100	1300	1500	1700	1900	2100	2300	2500
Effective crack- ing time (s)	751	626	573	381	400	363	360	263
Effective crack- ing gas pres- sure (MPa)	2.07	1.83	1.65	1.43	1.42	1.31	1.25	1.19

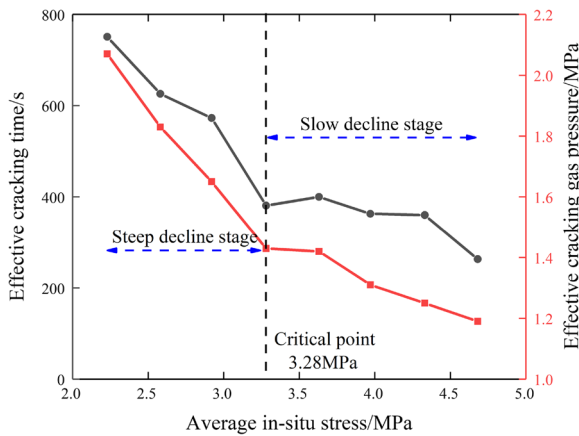


Fig. 5 Variation of effective cracking time and effective cracking gas pressure with average in-situ stress

$$K = \frac{(\sigma'_H + \sigma'_h)}{2\sigma'_v} \quad (3)$$

where, K is a dimensionless quantity denoting the lateral pressure coefficient of in-situ stress.

The variations in the effective cracking time and effective cracking gas pressure with average in-situ stress are shown in Fig. 5. As the average in-situ stress increases, the effective cracking time and effective cracking gas pressure exhibit a decreasing trend, indicating that under high in-situ stress conditions, coal is more likely to enter the sharp-fracture stage and present a risk of outburst. Preventive measures should be taken. With increases in depth, the change in the failure characteristic parameters of the coal obviously changes. To study the quantitative relationship between the effective cracking time and the effective cracking gas pressure with respect to the average in-situ stress, we take 3.28 MPa as the critical value (this is consistent with the critical depth of 1700 m in the Sect. 2). The changes in the coal failure characteristic parameters exhibit two distinct behaviors: a steep decline stage and a slow decline stage. On the steep decline stage, when the average in-situ stress is in the range 2.23–3.28 MPa, the effective cracking time and effective cracking gas pressure show a steep downward trend, with gradients of -352.38 s/MPa and 0.61 , respectively (that is, as the average in-situ stress increases by

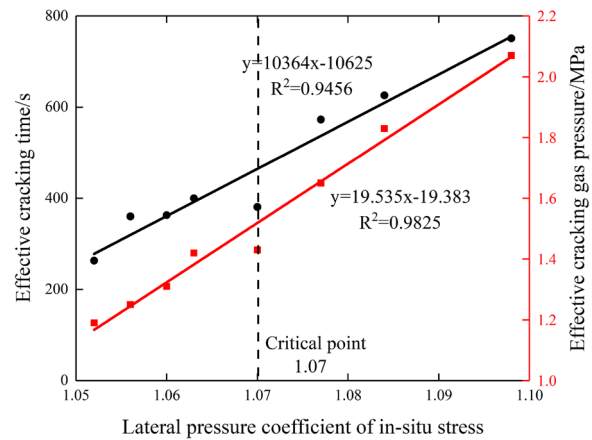


Fig. 6 Variation of effective cracking time and effective cracking gas pressure with the lateral pressure coefficient of in-situ stress

1 MPa, the time required for the coal to enter the sharp-fracture stage decreases by 352.38 s and the gas pressure decreases by 0.61 MPa). In the slow decline stage, when the average in-situ stress is from 3.28 to 4.68 MPa, the amplitudes of the effective cracking time and effective cracking gas pressure decrease with gradients of -84.29 s/MPa and 0.17 , respectively, some four times lower than in the steep decline stage.

The variations in the effective cracking time and effective cracking gas pressure with respect to the lateral pressure coefficient of in-situ stress are shown in Fig. 6. The effective cracking time and effective cracking gas pressure increase as the lateral pressure coefficient of in-situ stress increases, and the fitting relationship to a straight line is good (fitting coefficients are 0.9456 and 0.9825 respectively), indicating that there is a good linear relationship between the lateral pressure coefficient of in-situ stress and the coal failure characteristic parameters. Thus, this coefficient can be used as an important index for predicting the dynamic failure process of coal.

The variations in the effective cracking time and effective cracking gas pressure with respect to the critical gas pressure are shown in Fig. 7. The effective cracking time and the effective cracking gas pressure are positively correlated with the critical gas pressure. As the critical gas pressure increases, the time and gas pressure required for the coal to enter the sharp-fracture stage increase. For every 1 MPa increase in the

critical gas pressure, the effective cracking time and effective cracking gas pressure increase by 395.358 s and 0.743 MPa, respectively.

To measure the quantitative relationship between the effective cracking gas pressure and the critical gas pressure when the coal enters the sharp-fracture stage at different depths, the parameter W_p is defined. W_p represents the ratio of the effective cracking gas pressure to the critical gas pressure expressed as a percentage. That is,

$$W_p = \frac{P_q}{P_c} \times 100\% \tag{4}$$

where, P_q (MPa) denotes the effective cracking gas pressure at different depths and P_c (MPa) is the critical gas pressure at different depths. The variation of W_p with depth is shown in Fig. 8.

With increases in depth, the gas pressure at which the coal enters the sharp-fracture stage gradually decreases, indicating that the ratio between the effective cracking gas pressure and critical gas pressure is lower at greater depths. There is a logarithmic relationship between W_p and depth. Coal and gas outbursts can be predicted using abnormal gas pressures in the mine. When the depth reaches the critical value, slight changes in gas pressure will cause aggravated damage to the coal, which is more likely to cause intensive destruction and increase the outburst risk.

Effective stress is the combined effect of in-situ stress and gas pressure. Exploring the effective stress is of great significance for understanding the mechanism of deep coal and gas outbursts. Yi et al. (2007) deduced the following effective stress formula for deep mining:

$$\sigma_e = \frac{1}{3}(\sigma_v + \sigma_H + \sigma_h) - \frac{1}{2}(P_c - P_0) \tag{5}$$

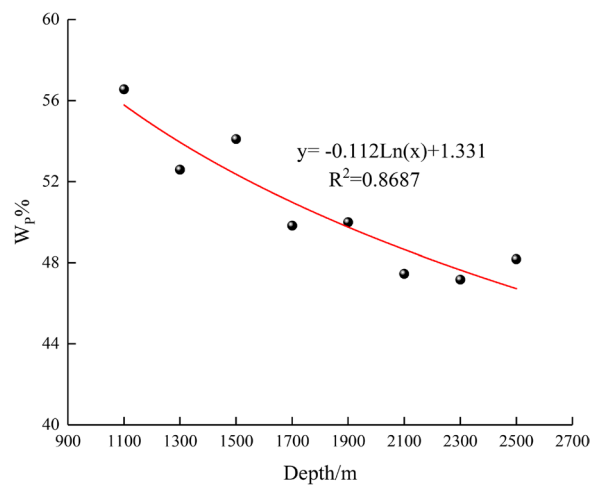


Fig. 8 Relationship between W_p and depth

where, σ_e (MPa) denotes the effective stress, σ_H (MPa) is the actual maximum horizontal in-situ stress, σ_h (MPa) is the actual maximum horizontal in-situ stress, and σ_v (MPa) is the actual vertical in-situ stress. P_0 is the standard atmospheric pressure of 0.1 MPa.

Based on the test results, the relationship between the effective stress and characteristic parameters of coal failure is shown in Fig. 9. Through the above analysis, it is clear that the effective cracking time and effective cracking gas pressure are negatively correlated with the average in-situ stress and positively correlated with the critical gas pressure. However, under the combined effect of in-situ stress and gas pressure, the overall behavior is a negative correlation, indicating that the effect of in-situ stress is greater than that of gas pressure in the process of outburst incubation. The related literature (Zhu et al. 2018) confirms this effect, suggesting that the experimental results are reasonable and feasible. As the effective stress increases, the time and the

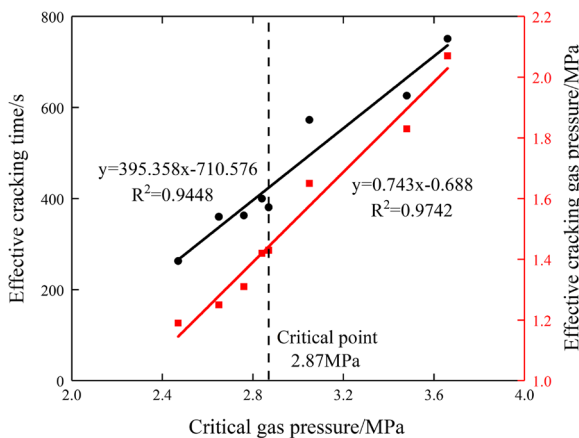


Fig. 7 Variation of effective cracking time and effective cracking gas pressure with critical gas pressure

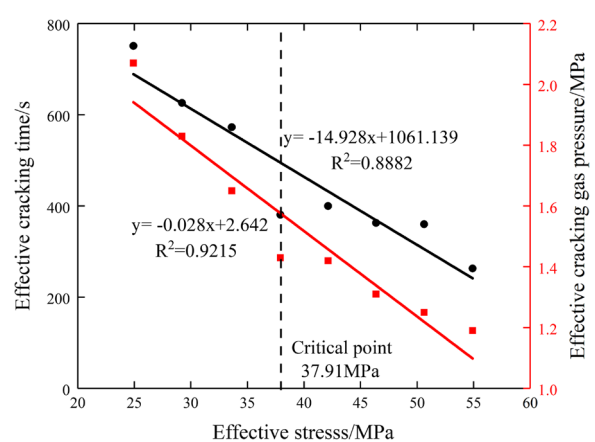


Fig. 9 Variation of effective cracking time and effective cracking gas pressure with effective stress

gas pressure required for the coal to enter the sharp-fracture stage decrease, meaning that coal and gas outburst accidents are more likely to occur.

Based on the above description, it can be seen that the effective cracking time and effective cracking gas pressure show staged changes with respect to the average in-situ stress and effective stress. When the average in-situ stress is greater than 3.28 MPa and the effective stress is greater than 37.91 MPa, the rates of change of the effective cracking time and effective cracking gas pressure slow down, indicating that the critical conditions of coal and gas outburst are sensitive to both the average in-situ stress and the effective stress. This means that slight changes once the average in-situ stress and effective stress have reached the critical value could cause accelerated destruction of the coal and early onset of the sharp-fracture stage, causing coal and gas outbursts.

3.3 Precursor risk index of gas outburst

The expansion multiple of the acoustic emission intensity from the microfracture stage to the sharp-fracture stage is defined as the outburst risk index N_1 :

$$N_1 = \frac{V_2}{V_1} \tag{6}$$

where, V_1 (mV) denotes the acoustic emission intensity per unit time in the microfracture stage and V_2 (mV) is the acoustic emission intensity per unit time in the sharp-fracture stage. The calculation results for different depths are presented in Table 6, and the relationship between N_1 and depth is shown in Fig. 10.

Under the experimental conditions, the risk index N_1 is between 3.74 and 9.54, and decreases as the depth increases. However, in different depth intervals, the variation of N_1 shows different distribution characteristics. Depending on the depth, the behavior of N_1 can be divided into two categories:

- (1) For depths of 1100–1700 m, N_1 is between 8.18 and 9.54. To effectively and accurately predict and prevent coal and gas outbursts, the outburst danger range is set to $N_1 \geq 7$. That is, when the depth is within the range 1100–1700 m, an increase in the acoustic emission intensity by a factor of more than 7 indicates that the

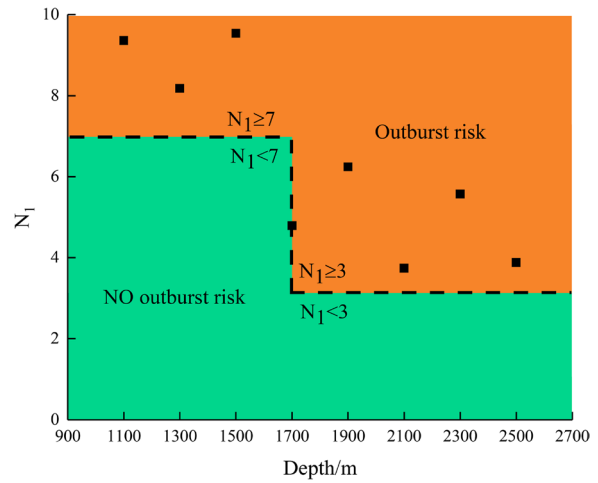


Fig. 10 Relationship between risk index N_1 and depth

- (2) For depths of 1700–2500 m, N_1 is between 3.74 and 6.24. To effectively and accurately predict and prevent coal and gas outbursts, the outburst danger range is set to $N_1 \geq 3$. That is, when the depth is within the range 1700–2500 m, an increase in the acoustic emission intensity by more than a factor of 3 indicates that the coal has entered the sharp-fracture stage. The maximum depth considered in the tests is 2500 m. At greater depths, the outburst danger range for N_1 is likely to be less than 3.

It can be seen from the distribution characteristics of the risk index N_1 that, as the depth increases, the acoustic emission transition from no outburst risk to outburst risk becomes less obvious, indicating the sudden and unpredictable characteristics of deep coal and gas outbursts. Therefore, it is particularly important to study the precursor information and outburst prediction indicators of deep coal and gas outbursts. The outburst precursor risk index can clearly distinguish whether the coal seam is at risk of outburst. The outburst risk index proposed in this paper is based on laboratory tests of coal samples from Hongyang No. 3 mine, and the universality of its practical application requires further study.

Table 6 Outburst risk index at different depths

Depth (m)	1100	1300	1500	1700	1900	2100	2300	2500	Actual data
V_1 (mV)	8.54	5.61	10.74	6.05	21.40	18.76	18.54	13.27	10
V_2 (mV)	79.96	45.89	102.49	50.34	133.63	70.27	103.37	51.49	60
N_1	9.36	8.18	9.54	8.32	6.24	3.74	5.57	3.88	6

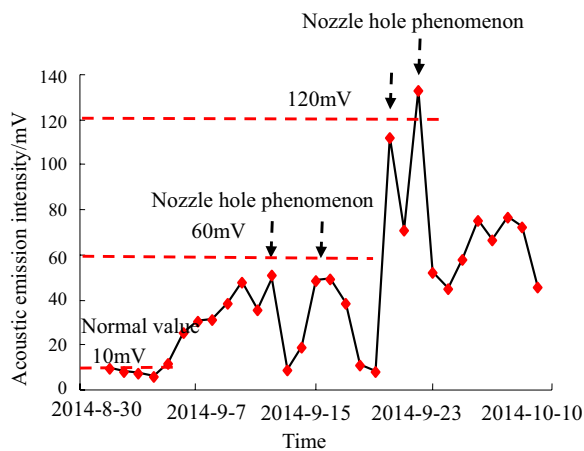


Fig. 11 Acoustic emission parameters measured in Yizhong coal mine

4 Test verification

The test results are now compared with measured acoustic emission intensities from Yizhong coal mine. The acoustic emission intensities measured at 11,112 tunneling face (depth of 1705 m) in Yizhong coal mine from August 30–October 10, 2014, are shown in Fig. 11 (Chen 2016). During the tunneling process, the acoustic emission intensity increases in a step-wise manner. When the acoustic emission intensity is at 10 mV, the working face is relatively stable and has no tendency to protrude. When the acoustic emission intensity surges by a factor of 6 and reaches 60 mV, the conventional index exceeds the standard or the nozzle hole phenomenon occurs, indicating a higher risk of coal seam outburst. When the acoustic emission intensity increases to 120 mV, the conventional index exceeds the standard or the nozzle hole phenomenon again occurs. The acoustic emission intensity growth trend is similar to the results obtained in this article, and the acoustic emission intensity monitoring results are at the same numerical level as the data presented in this paper. As shown in Table 6, the measured data from Yizhong coal mine give an outburst risk index of $N_1 = 6$ and the coal seam depth is greater than 1700 m. This indicates a dangerous outburst risk, indicating that the test results are reasonable. However, due to the limitations of the test conditions, the universality of the outburst risk index N_1 requires further study.

The application of acoustic emission monitoring technology in the 11,112 tunneling face of Yizhong coal mine shows that acoustic emission monitoring can be applied for effective real-time monitoring of the dynamic change process of coal seams. This paper has analyzed the correlation between coal destruction and acoustic emission parameters during coal and gas outburst through laboratory test methods. According to the acoustic emission parameters, a

prediction index for coal and gas outburst was proposed. The results presented herein are intended to provide scientific reference for further studies on coal and gas outburst.

5 Conclusions

- (1) Acoustic emission signals from tests at different depths have been analyzed, and the process of gas tearing the coal has been divided into two parts: the microfracture stage and the sharp-fracture stage. When the coal enters the sharp-fracture stage under the action of gas pressure, the internal damage of the coal has increased and there is a risk of outburst.
- (2) The effects of the average in-situ stress, lateral pressure coefficient of in-situ stress, critical gas pressure, and effective stress on coal failure characteristic parameters were analyzed, and the coal damage was found to exhibit step-wise changes. To accurately predict and prevent deep coal and gas outburst disasters, targeted coal and gas outburst precursor indicators for different depths were formulated, and segmented evaluations were conducted to improve the prediction accuracy.
- (3) Based on variations in the acoustic emission intensity per unit time, the expansion multiple of acoustic emission intensity from the microfracture stage to the sharp-fracture stage of coal was defined as the outburst risk index N_1 . The N_1 risk range is defined according to depth. The critical depth between deep and shallow coal is 1700 m. When the depth is from 1100 to 1700 m, $N_1 \geq 7$, whereas from 1700 to 2500 m, $N_1 \geq 3$. At greater depths, the outburst risk index takes a smaller value, indicating that the coal is more likely to suffer an outburst event.

Acknowledgements This research was financially supported by the National Natural Science Foundation of China (51874165, 51974148), and Liaoning Xingliao Talent Program (XLYC1902106).

Authors' contributions All authors read and approved the final manuscript.

Declarations

Conflict of interest The authors declare that they have no conflict of interest.

Human and animal rights This article does not contain any studies with human participants or animals performed by any of the authors.

Informed consent Informed consent was obtained from all individual participants included in the study.

Open Access This article is licensed under a Creative Commons Attribution 4.0 International License, which permits use, sharing, adaptation, distribution and reproduction in any medium or format, as long as you give appropriate credit to the original author(s) and the source, provide a link to the Creative Commons licence, and indicate if changes were made. The images or other third party material in this article are included in the article's Creative Commons licence, unless indicated otherwise in a credit line to the material. If material is not included in the article's Creative Commons licence and your intended use is not permitted by statutory regulation or exceeds the permitted use, you will need to obtain permission directly from the copyright holder. To view a copy of this licence, visit <http://creativecommons.org/licenses/by/4.0/>.

References

- Alekseev AD, Nedodayev NV, Starikov GP (1980) Destruction of coal saturated with gas under triaxial stress field on destressing: Modeling of outbursts of coal and gas. *Inst Probl Mekhaniki USSR* 139:30
- Cao J, Dai LC, Sun HT, Wang B, Zhao B, Yang XL, Zhao XS, Guo P (2019) Experimental study of the impact of gas adsorption on coal and gas outburst dynamic effects. *Process Saf Environ* 128:158–166
- Cao WZ, Shi JQ, Durucan S, Si GY, Korre A (2020) Gas-driven rapid fracture propagation under unloading conditions in coal and gas outbursts. *Int J Rock Mech Min Sci* 130:104325
- Chen L (2016) Research on real-time monitoring & early warning technology of coal and gas outburst of the driving working face. China University of Mining and Technology, Xuzhou ((in Chinese))
- Chen YP, Liu HY, Zhao W (2014) Status and prevention countermeasures of coal and gas outburst accidents in China. *Coal Sci Technol* 42(6):15–18 ((in Chinese))
- Fu G, Xie XC, Jia QS, Tong WQ, Ge Y (2019) Accidents analysis and prevention of coal and gas outburst: understanding human errors in accidents. *Process Saf Environ Prot* 134:1–23
- Guo DY, Lv PF, Zhao JC, Zhang C (2020) Research progress on permeability improvement mechanisms and technologies of coalbed deep-hole cumulative blasting. *Int J Coal Sci Technol* 7(2):329–336
- Heo JS, Lee CI, Jeon SK (2004) Measurement of acoustic emission and source location considering anisotropy of rock under triaxial compression. *Key Eng Mater* 270–273:1574–1579
- Hu QT, Zhou SN, Zhou XQ (2008) Mechanical mechanism of coal and gas outburst process. *J China Coal Soc* 33(12):1368–1372 ((in Chinese))
- Hu YY, Hu XM, Zhang QT, Zhu SH (2012) Analysis on simulation experiment of outburst in uncovering coal seam in cross-cut. *Procedia Eng* 45:287–293
- Jiang FX (2015) Technology and application of high-gas and low through coal seam hydraulic fracturing rock cross-cut coal uncovering. Anhui University of Science and Technology, Huainan ((in Chinese))
- Jiang CL, Yu QX (1995) Spherical shell destabilization hypothesis of coal and methane outburst mechanism. *Saf Coal Mines* 2:17–25 ((in Chinese))
- Li XP, Wang B, Zhou GL (2012) Research on distribution rule of geostress in deep stratum in Chinese mainland. *Chin J Rock Mech Eng* 31(S1):2875–2880 ((in Chinese))
- Li LL, Tang JP, Sun SJ, Ding JH (2019) Experimental study of the influence of water content on energy conversion of coal and gas outburst. *Nat Hazards* 97:1083–1097
- Liu QL, Wang EY, Kong XG, Li Qing HuSB, Li DX (2018) Numerical simulation on the coupling law of stress and gas pressure in the uncovering tectonic coal by cross-cut. *Int J Rock Mech Min* 103:33–42
- Lu CP, Dou LM, Zhang N, Xue JH, Liu GJ (2014) Microseismic and acoustic emission effect on gas outburst hazard triggered by shock wave: a case study. *Nat Hazards* 73(3):1715–1731
- Ma YK, Nie BS, He XQ, Li XC, Meng JQ, Song DZ (2020a) Mechanism investigation on coal and gas outburst: an overview. *Int J Miner Metall Mater* 27(7):872–887
- Ma YK, He XQ, Li ZH (2020b) A unified model with solid-fluid transition for coal and gas outburst and FEMLIP modeling. *Tunn Undergr Space Technol* 99:103349
- Nie BS, Ma YK, Hu ST, Meng JQ (2019) Laboratory study phenomenon of coal and gas outburst based on a mid-scale simulation system. *Sci Rep* 9(1):15005
- Peng SJ, Xu J, Yang HW, Liu D (2012) Experimental study on the influence mechanism of gas seepage on coal and gas outburst disaster. *Saf Sci* 50(4):816–821
- Singh JG (1984) A mechanism of outbursts of coal and gas. *Min Sci Technol* 1(4):269–273
- Tang JP (2006) Theoretical and experimental research of storage and transport of coalbed methane by NMR technique. Liaoning Technical University, Fuxin
- Tang JP, Pan YS, Yang SL (2013) Experimental study of coal and gas outburst under tridimensional stresses. *Chin J Rock Mech Eng* 32(5):960–965 ((in Chinese))
- Wang X, Meng FB (2018) Statistical analysis of large accidents in China's coal mines in 2016. *Nat Hazards* 92:311–325
- Wang HF, Chen YP, Yuan L (2013) Gas outburst disasters and the mining technology of key protective seam in coal seam group in the Huainan coalfield. *Nat Hazards* 67(2):763–782
- Wu X, Peng YW, Xu J, Yan Q, Nie W, Zhang TT (2020) Experimental study on evolution law for particle breakage during coal and gas outburst. *Int J Coal Sci Technol* 7(1):97–106
- Xie XG, Feng T (2011) Research on numerical simulation of freezing temperature field in uncovering outburst coal seam in cross-cut. *J China Coal Soc* 36(9):1511–1514 ((in Chinese))
- Xu J, Liu D, Yin G, Lu Q, Peng S (2012) Simulation experiment of coal and gas outburst under non-uniform load. *J China Coal Soc* 37:836–842
- Xue Y, Gao F, Liu XG (2015) Effect of damage evolution of coal on permeability variation and analysis of gas outburst hazard with coal mining. *Nat Hazards* 79:999–1013
- Yang DD, Chen YJ, Tang J, Jiang CL (2021) Comparative experimental study of methods to predict outburst risk when uncovering coal in crosscuts. *Fuel* 288:119851
- Yi J, Jiang YD, Xian XF (2007) An experimental research on the characters of methane seepage in stress field and temperature field. *China Min Mag* 16(5):113–116 ((in Chinese))
- Yu BH, Su CX, Wang DM (2015) Study of the features of outburst caused by rock cross-cut coal uncovering and the law of gas dilatation energy release. *Int J Min Sci Technol* 25(3):453–458
- Yuan L, Wang W, Wang HP, Zhang B, Liu ZZ, Yu GF, Zuo YJ (2020) Simulation test system for inducing coal and gas outburst in roadway driving. *J China Univ Min Technol* 49(2):205–214 ((in Chinese))
- Zhang CL, Wang EY, Xu J, Peng SJ (2021) A new method for coal and gas outburst prediction and prevention based on the fragmentation of ejected coal. *Fuel* 287:119493
- Zhao ZQ, Jin JX, Shen JC (2019) Promotion characteristics and induced outburst mechanisms of coal plastic zones in rock cross-cut coal uncovering. *Chin J Rock Mech Eng* 38(2):343–352 ((in Chinese))
- Zhao W, Wang K, Zhang R, Dong HZ, Lou Z, An FH (2020) Influence of combination forms of intact sub-layer and tectonically deformed sub-layer of coal on the gas drainage performance of boreholes: a numerical study. *Int J Coal Sci Technol* 7(3):571–580

Zhou AT, Zhang M, Wang K, Elsworth D (2020) Near-source characteristics of two-phase gas–solid outbursts in roadways. *Int J Coal Sci Technol* 8(5):685–696

Zhu LK, Yang TH, Xu T, Zhao GH, Xie ZH (2018) Explore the mechanism of ground stress and gas pressure in coal-gas outburst. *J Min Saf Eng* 35(5):1038–1044 (**in Chinese**)